Journal of Magnetic Resonance **144,** 123–128 (2000)
doi:10.1006/jmre.2000.2020, available online at http://www.idealibrary.com on IDEAL®

Clean TROSY: Compensation for Relaxation-Induced Artifacts[1]

Thomas Schulte-Herbrüggen and Ole Winneche Sørensen

Department of Chemistry, Carlsberg Laboratory, Gamle Carlsberg Vej 10, DK-2500 Valby, Denmark

Received September 22, 1999; revised December 27, 1999

TROSY pulse sequences for recording, e.g., ^{1}H–^{15}N chemical shift correlation spectra of proteins are designed to select only one of four two-dimensional multiplet components. However, all of the variants published so far are prone to relaxation-induced artifacts at the positions of two of the other multiplet components. This article introduces modifications to the two spin-state-selective coherence transfer building blocks of the TROSY mixing sequence resulting in a clean TROSY spectrum with the artifacts largely suppressed. It works by having the new mixing sequence generate peaks of opposite phase at the positions of the relaxation artifacts. The clean TROSY pulse sequence is marginally shorter than the original one and contains the same pulses. Experimental demonstration is presented for the ^{15}N-labeled proteins RAP 17–97 (N-terminal domain of α_2-macroglobulin receptor associated protein) and EQT, equinatoxin II, from the Mediterranean anemone *Actinia equina.*

Key Words: **multidimensional NMR; clean TROSY; S^{3}CT.**

Recording heteronuclear correlation spectra of large molecules at high magnetic fields without heteronuclear decoupling can enhance both resolution and sensitivity (*1*) as has been demonstrated recently in terms of the so-called TROSY approach applied to ^{1}H–^{15}N (*2*) and ^{1}H–^{13}C (*3*) correlations in proteins. One of four two-dimensional (2D) multiplet components benefits from favorable subtractive interference between dipolar and chemical shift anisotropy relaxation mechanisms causing a relatively long transverse relaxation time for that component while the other three peaks are broader (*4*).

The latter ones are of no value in heteronuclear chemical shift correlation spectra recorded without heteronuclear decoupling. Hence it was suggested that special pulse sequences designed to suppress them be applied, thus resulting in spectra with only the narrow peak (*2*). However, Rance *et al.* (*5*) have shown that these TROSY pulse sequences are prone to relaxation-induced artifacts at the positions of the broader components. Clearly, it is desirable to modify the TROSY pulse sequences to suppress these artifacts as they might interfere with real TROSY peaks and lead to spectral ambiguities. That is the issue addressed in this paper and it will be shown that such modifications are indeed possible so that clean TROSY spectra can be obtained.

The idea is to modify the two spin-state-selective coherence transfer (S^{3}CT) building blocks (*6, 7*) of the TROSY mixing sequence so as to compensate for the relaxation-induced artifacts by coherently generating exactly the same artifacts but with opposite phase. The same idea has been applied earlier to another simpler problem of relaxation-induced artifacts interfering with measurement of J coupling constants (*8*). The modifications to the two S^{3}CT elements shall be derived in analogy to an earlier improvement to the TROSY pulse sequence (*7*). But first the nomenclature of TROSY, anti-TROSY, and F_1 or F_2 semi-TROSY peaks is defined in Fig. 1. The relaxation artifacts occur at the positions of the semi-TROSY peaks (*5*).

Disregarding signs of frequencies, the echo and antiecho 2D TROSY peaks in an ^{15}N–^{1}H system occur as the high-frequency doublet component in the ^{15}N dimension and as the low-frequency doublet component in the ^{1}H dimension. Hence, as the gyromagnetic ratios for ^{15}N and ^{1}H are negative and positive, respectively (i.e., positive and negative Larmor frequencies, respectively), and the ^1J coupling constant is negative, the TROSY peak coordinates are $(\Omega_N - \pi J, \Omega_H - \pi J)$ in the echo and $(-\Omega_N + \pi J, \Omega_H - \pi J)$ in the antiecho. Thus the pertinent coherence transfers for the clean TROSY mixing sequence are

$$I^\beta S^\pm \nearrow I^- S^\beta \quad \searrow I^- S^\alpha \qquad [1a]$$

$$I^\alpha S^\pm \dashrightarrow I^- S^\beta, \qquad [1b]$$

where the solid line indicates the transfer for the desired TROSY peak whereas the dashed lines represent those leading to the semi-TROSY peaks. As shown in Ref. (*7*) two consecutive S^{3}CT elements yield the desired TROSY coherence transfers, e.g., for the echo part:

$$I^\beta S^- \xrightarrow[(1)]{\pi I_y S^\alpha} I^- S^- \xrightarrow[(2)]{\pi I^\alpha S_y} I^- S^\beta. \qquad [2]$$

[1] Presented in part at the Nordic NMR Symposium, Gothenburg, Sweden, August 24–25, 1999.

1090-7807/00 $35.00

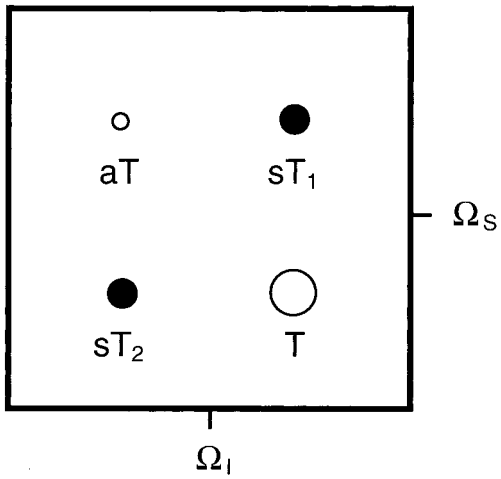

FIG. 1. Schematic ^{15}N–^{1}H TROSY multiplet pattern (antiecho). The desired component, dubbed "TROSY peak," is marked with a T, whereas the artifacts comprise the two "semi-TROSY peaks" in F_1 (sT_1) and F_2 (sT_2), respectively, as well as the so-called "anti-TROSY peak" labeled aT. In the uncompensated original TROSY experiment, the semi-TROSY peaks arising from different single- versus multiple-quantum relaxation rates (*5*) have opposite phase of the TROSY peak while the anti-TROSY peak is most often not visible due to much lower amplitude and fast decay.

But in order to open the other pathways in Eq. [1] it is necessary to let these two rotation angles deviate from π and to include small rotations on the respective other doublet transitions, i.e., those with the passive spin in the β state. In other words, the first and second S^{3}CT elements are replaced by

$$p_I \pi I_y S^{\alpha} + q_I \pi I_y S^{\beta} \qquad [3a]$$

and

$$p_S \pi I^{\alpha} S_y + q_S \pi I^{\beta} S_y, \qquad [3b]$$

respectively, where in the absence of the relaxation effects $p_I = p_S = 1$ and $q_I = q_S = 0$, i.e., as in Eq. [2]. These rotations are illustrated in Fig. 2 and the resulting peak-intensity patterns as they occur in ^{15}N–^{1}H TROSY are shown in Fig. 3. The intensities can be derived from the diagrams in Fig. 2 and the following two transformation formulas for single-transition operators

$$e^{-i\Psi I_y^{s,t}} I_{r,s}^{\pm} e^{i\Psi I_y^{s,t}} = I_{r,s}^{\pm} \cos\frac{\Psi}{2} + I_{r,t}^{\pm} \sin\frac{\Psi}{2} \qquad [4a]$$

$$e^{-i\Psi I_y^{r,t}} I_{r,s}^{\pm} e^{i\Psi I_y^{r,t}} = I_{r,s}^{\pm} \cos\frac{\Psi}{2} + I_{t,s}^{\pm} \sin\frac{\Psi}{2}, \qquad [4b]$$

where indices r, s, and t refer to three different energy levels.

For the conversion of the two modified S^{3}CT rotations into pulse sequences it is convenient to introduce new variables:

$$\phi_I = (p_I + q_I)\pi/2 \qquad [5a]$$

$$\phi_S = (p_S + q_S)\pi/2 \qquad [5b]$$

$$\theta_I = (p_I - q_I)\pi/2 \qquad [5c]$$

$$\theta_S = (p_S - q_S)\pi/2. \qquad [5d]$$

Hence the combined propagator of Eq. [3] can be rearranged according to

$$\begin{aligned} & e^{i\phi_I I_y} e^{i\theta_I 2I_y S_z} e^{i\theta_S 2I_z S_y} e^{i\phi_S S_y} \\ &= e^{-i\pi I_z} e^{i\pi I_z} e^{i\phi_I I_y} e^{-i(\pi/2)I_x} e^{-i(\theta_I/2)2I_z S_z} e^{i\pi(I_y+S_y)} e^{-i\pi(I_y+S_y)} \\ &\quad \times e^{-i(\theta_I/2)2I_z S_z} e^{i\pi(I_y+S_y)} e^{-i(\pi/2)I_x} e^{i(\pi/2)S_x} e^{-i\pi(I_y+S_y)} \\ &\quad \times e^{-i(\theta_S/2)2I_z S_z} e^{i\pi(I_y+S_y)} e^{-i\pi(I_y+S_y)} e^{-i(\theta_S/2)2I_z S_z} \\ &\quad \times e^{i(\pi/2)S_x} e^{i\phi_S S_y} e^{-i\pi I_z} e^{i\pi I_z} \\ &= e^{-i(\pi+\phi_I)I_z} \{ e^{i\phi_I I_z} e^{i(\pi/2)I_x} e^{-i\phi_I I_z} \} e^{-i(\theta_I/2)2I_z S_z} e^{i\pi(-I_y+S_y)} \\ &\quad \times e^{-i(\theta_I/2)2I_z S_z} e^{i(\pi/2)I_x} e^{i(\pi/2)S_x} e^{-i(\theta_S/2)2I_z S_z} e^{i\pi(I_y-S_y)} \\ &\quad \times e^{-i(\theta_S/2)2I_z S_z} \{ e^{-i\phi_S S_z} e^{i(\pi/2)S_x} e^{i\phi_S S_z} \} e^{-i\phi_S S_z} e^{i\pi I_z}, \end{aligned} \qquad [6]$$

where the z rotations outside the braces in the final expression can be omitted as they have no influence on the spectrum, and the propagators in the two braces represent $\pi/2$ pulses on I (phase $-\phi_I$) and S (phase ϕ_S), respectively. The negative signs on the angles in the terms with $2I_zS_z$ are prepared for the fact that J is negative for ^{15}N–^{1}H systems.

However, before converting Eq. [6] to an actual pulse sequence it is necessary to pay attention to the jungle of signs in NMR (*9*). Levitt has pointed out that current NMR instruments do not distinguish between spins with positive and negative gyromagnetic ratios when RF pulses are phase shifted and that this must be considered in the spin dynamics (*9*). The consequence is that the γ-sensitive phase shifts on ^{15}N and ^{1}H channels of current NMR spectrometers are in opposite sense (*9*). This means that one of the phases ϕ_I or ϕ_S must be inverted. Which one it is depends on the sense of the actual RF phase shifts on the instruments and that is opposite on Varian and Bruker spectrometers. In order not to make this a problem in practical applications we introduce new phases φ_I and φ_S instead of $-\phi_I$ and ϕ_S and implement the pulse sequence as outlined in Fig. 4a. Furthermore, for the applications in mind the results are insensitive to π phase shifts of π pulses.

As is obvious in Fig. 2 the other coherence transfers in Eq. [1] starting with $I^{\beta}S^{+}$ and $I^{\alpha}S^{+}$ amount to permutation of p_I with q_I and p_S with q_S, or in other words sign inversion of θ_I and θ_S. Hence, due to the equality

$$\begin{aligned} & e^{i\phi_I I_y} e^{-i\theta_I 2I_y S_z} e^{-i\theta_S 2I_z S_y} e^{i\phi_S S_y} \\ &\quad = e^{-i\pi(I_z+S_z)} e^{-i\phi_I I_y} e^{i\theta_I 2I_y S_z} e^{i\theta_S 2I_z S_y} e^{-i\phi_S S_y} e^{i\pi(I_z+S_z)}, \end{aligned} \qquad [7]$$

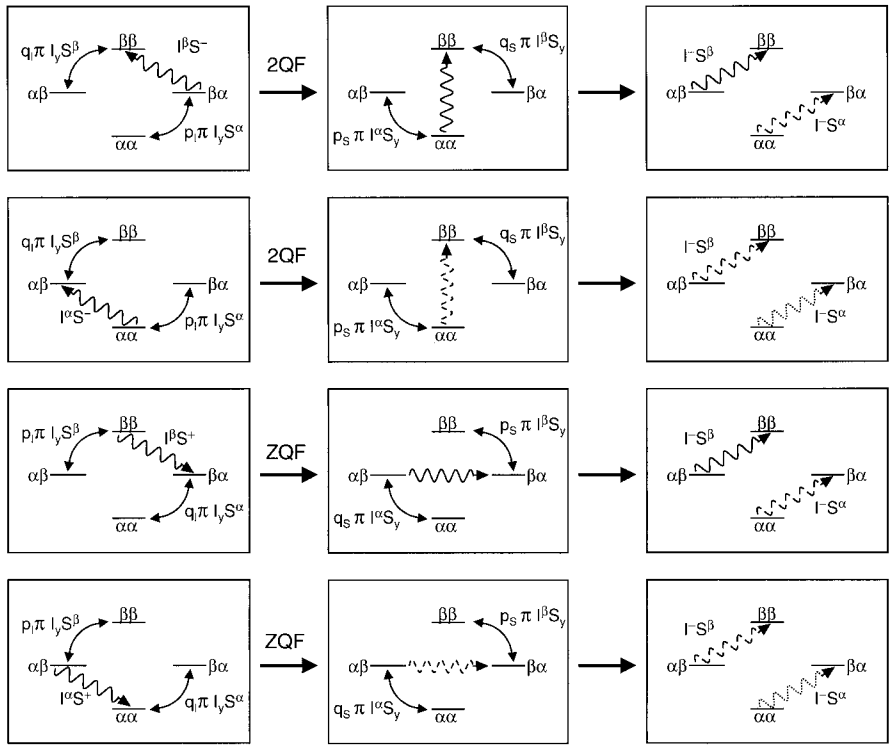

FIG. 2. Coherence transfer processes needed for clean TROSY. In an idealized uncompensated TROSY mixing process (corresponding to $p_I = p_S = 1$, $q_I = q_S = 0$) two consecutive spin-state-selective π rotations (*7*) take the coherence $I^{\beta}S^{-}$ (or $I^{\beta}S^{+}$) to $I^{-}S^{\beta}$ thus giving rise to a single multiplet component—the TROSY peak (solid wavy lines)—in the 2D IS multiplet (cf., Fig. 1). Semi-TROSY peaks (dashed lines) can be generated with well-controllable amplitudes (given in Fig. 3 for ^{15}N–^{1}H TROSY) if the spin-state-selectivity is lifted, i.e., when q_I or q_S differ from zero. Anti-TROSY peaks (dotted lines) have negligible intensity.

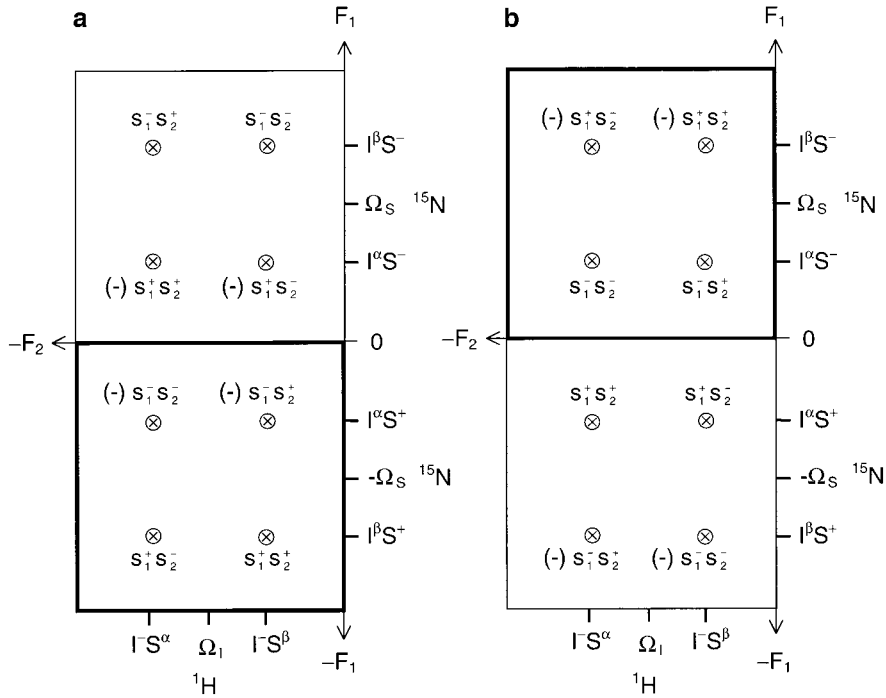

FIG. 3. Intensities of the multiplet components in a generalized ^{15}N–^{1}H TROSY spectrum allowing for all the spin-state-selective rotations shown in Fig. 2. The negative signs in brackets reflect the antiphase character of the preparation sequence and not the TROSY mixing sequence. Antiecho and echo are framed in bold in (a) and (b), respectively. The intensity expressions are abbreviated $s_I^{\pm}s_S^{\pm} = -\frac{1}{4}\{\sin\theta_I \pm \sin\varphi_I\}\{\sin\theta_S \pm \sin\varphi_S\}$. For example, the intensity for the TROSY peaks is easily calculated from Eq. [4]: $\sin(p_I\pi/2)\cos(q_I\pi/2) \times \sin(p_S\pi/2)\cos(q_S\pi/2)$, which can be rearranged according to Eq. [5].

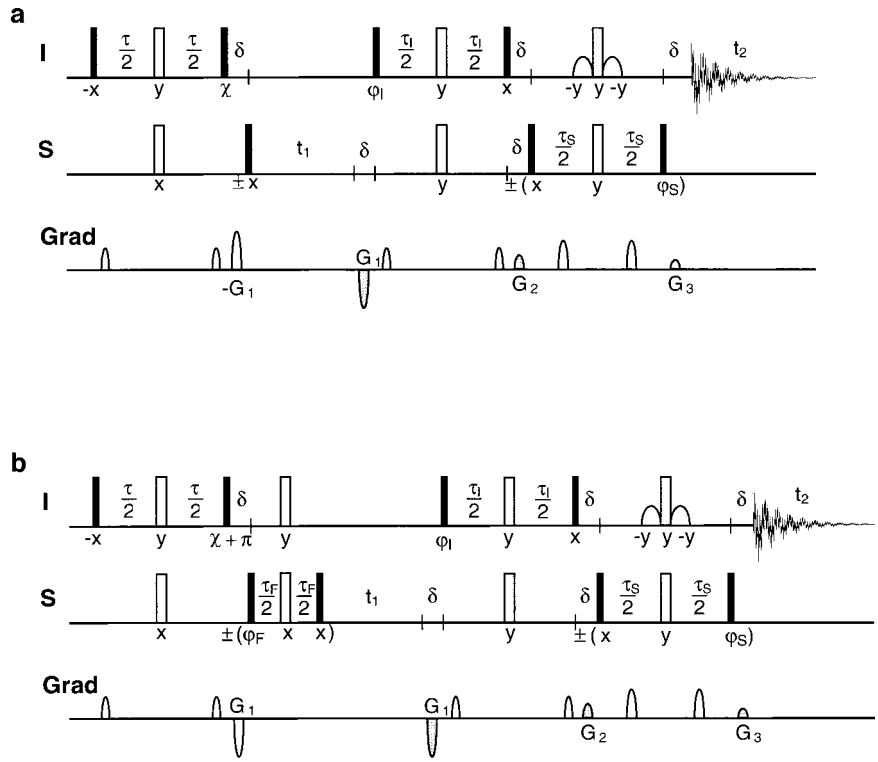

FIG. 4. Clean TROSY pulse sequences without (a) and with S^3E filter (b). For ^{15}N–^{1}H correlation on Bruker instruments, phases $\varphi_I = -y$, $\varphi_S = -y - \Delta\varphi_S$, and gradient ratios $(G_1{:}G_2{:}G_3) = (-7{:}3{:}1.987)$ select the echo, whereas the setting $\varphi_I = y$, $\varphi_S = y - \Delta\varphi_S$, and $(G_1{:}G_2{:}G_3) = (-8{:}2{:}3.013)$ selects the antiecho. On Varian instruments the φ_I and φ_S phases must be inverted. In order to include the native ^{15}N magnetization, χ is y and $-y$ on Bruker and Varian instruments, respectively. The prefix $\pm$ to pulse phases indicates independent π phase shift two-step cycles with alternating receiver phase. The delays are $\tau = \tau_S = (2J_{NH})^{-1}$ and $\tau_I = (2J_{NH})^{-1} - \Delta\tau_I$. The uncompensated TROSY experiment employs $\Delta\varphi_S = \Delta\tau_I = 0$. The clean TROSY sequence with the S^3E filter shown in (b) eliminates F_1 semi-TROSY artifacts by the preparation sequence. Phase cycling and gradient settings are the same as in (a) except for the sign in the first of the two G_1 gradients.

it follows that the corresponding pulse sequence can be realized as the one for the transfers starting from $I^{\beta}S^{-}$ and $I^{\alpha}S^{-}$ by inverting the signs of ϕ_I and ϕ_S or equivalently of φ_I and φ_S. Alternatively, π can be added to these two phases (vide infra, Eq. [8]).

The relaxation-induced F_1 and F_2 semi-TROSY artifacts occur with opposite phase to the TROSY peak (*5*), so the compensating coherence transfers must generate peaks of the same phase as the TROSY peak. Hence according to Fig. 3 the equations relevant for the problem read

$$f_{\mathrm{TROSY}} = \tfrac{1}{4}\{\sin\theta_I + \sin\phi_I\}\{\sin\theta_S + \sin\phi_S\} \qquad [8a]$$

$$f_1 = -\tfrac{1}{4}\{\sin\theta_I - \sin\phi_I\}\{\sin\theta_S + \sin\phi_S\} \qquad [8b]$$

$$f_2 = \tfrac{1}{4}\{\sin\theta_I + \sin\phi_I\}\{\sin\theta_S - \sin\phi_S\}, \qquad [8c]$$

where the TROSY peak intensity is to be maximized subject to the boundary conditions that semi-TROSY peaks of intensities f_1 and f_2, respectively, must be generated. The negative sign in Eq. [8b] arises from the π phase shift of the associated coherence after the initial INEPT (antiphase) transfer. The solution for the usual case of $f_1 > f_2$ (*5*) is

$$\phi_I = \theta_S = \pi/2 \qquad [9a]$$

$$\sin\theta_I = \sqrt{(f_1 - f_2)^2 - 2(f_1 + f_2) + 1} - (f_1 - f_2) \qquad [9b]$$

$$\sin\phi_S = \sqrt{(f_1 - f_2)^2 - 2(f_1 + f_2) + 1} + (f_1 - f_2) \qquad [9c]$$

$$f_{\mathrm{TROSY}} = \tfrac{1}{2}\{1 - (f_1 + f_2) + \sqrt{(f_1 - f_2)^2 - 2(f_1 + f_2) + 1}\}. \qquad [9d]$$

Note that the above equations do not consider possible concomitant amplitude changes in the multiplet components caused by relaxation changes in the modified pulse sequence.

A typical example resulting in clean TROSY spectra is $f_1 = 0.05$ and $f_2 = 0.01$ requiring $\theta_I = 64°$ and $\phi_S = 78°$; this leads to $f_{\mathrm{TROSY}} = 0.94$, i.e., a modest 6% sensitivity penalty for suppression of the relaxation-induced artifacts. In practice, we

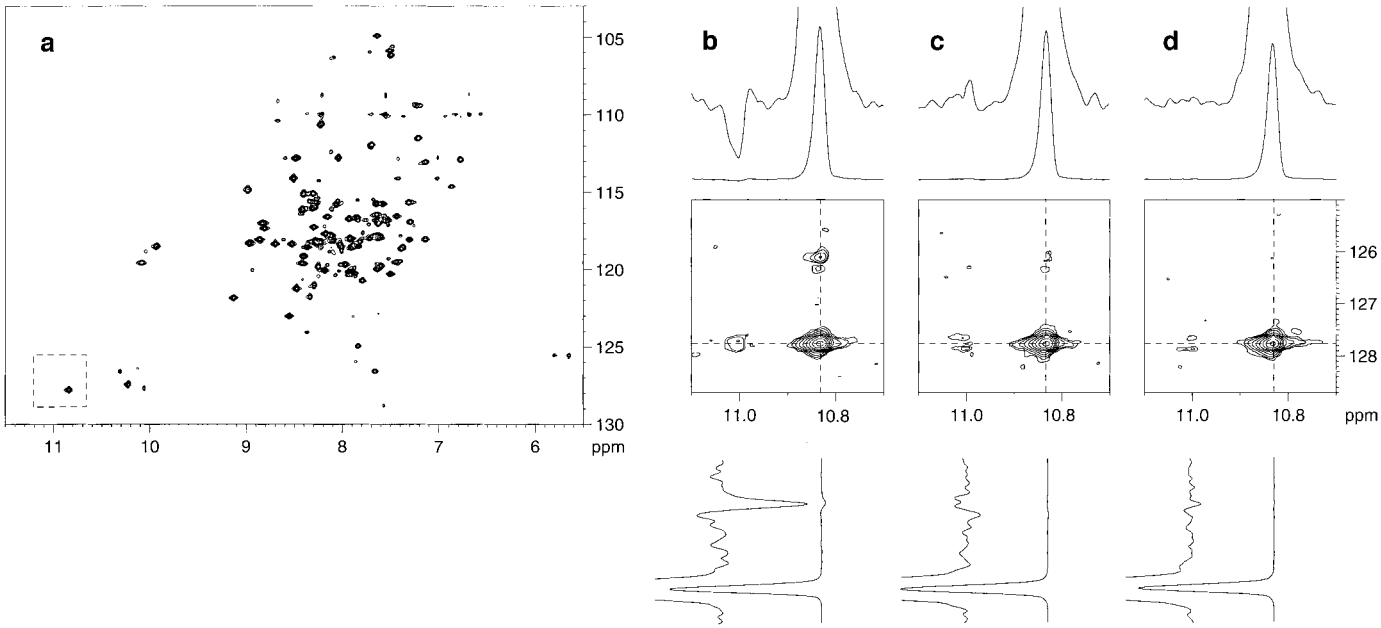

FIG. 5. ^{15}N–^{1}H clean TROSY of the ^{15}N-labeled α_2-macroglobulin associated protein (RAP 17-97; 90%/10% H_2O/D_2O, 300 K, pH 6.4) recorded with the pulse sequence in Fig. 4a on a Bruker DRX 600-MHz spectrometer. The dashed region in the overview (a) is expanded: (b) shows the prominent semi-TROSY artifacts of the conventional TROSY spectrum, i.e., recorded with the pulse sequence of Fig. 4a with the parameters $\tau = \tau_I = \tau_S = (2J_{NH})^{-1} = 5.05$ ms (with $J_{NH} = 99$ Hz for the tryptophan indoles) and $\varphi_I = \varphi_S = \pm y$ in the antiecho/echo selection. The clean TROSY spectrum shown in (c) was obtained using the parameters $\tau = \tau_S = (2J_{NH})^{-1} = 5.05$ ms and $\tau_I = 3.37$ ms (i.e., $\theta_I = \pi J_{NH}\tau_I = 60°$ or $\Delta\theta_I = 30°$) and $\varphi_I = \pm y$ and $\varphi_S = 80°, -100°$ (i.e., $\Delta\varphi_S = 10°$) for antiecho/echo selection. (d) presents a clean TROSY spectrum recorded with the sequence of Fig. 4b with the S^3E-type filter prior to t_1 and the setting $\tau_F = 2.24$ ms and $\varphi_F = 50°$. The other parameters are $\tau_I = \tau_S = (2J_{NH})^{-1}$, $\varphi_I = \pm y$ and $\varphi_S = 80°, -100°$. In all cases 8 scans were recorded with 512 echo and 512 antiecho increments in t_1 and 2048 data points in t_2 in the conventional alternating antiecho/echo mode. Spectral widths were 15 ppm in F_2 (centered at the water resonance) and 50 ppm in F_1. Zero-filling to 8k (t_2) by 4k (t_1) data points prior to strip transformation was done for the spectral regions shown while apodization employed a $\cos^2$ window function shifted by 18° in both dimensions. Finally, the Watergate elements employed Gaussian water-selective $\pi/2$ pulses of 750-μs duration.

have noticed the opposite, namely a slight, sensitivity enhancement due to the shorter delay in the first S^3CT element of the TROSY mixing sequence.

The key experimental parameters can be written

$$\tau_I = \frac{1}{\pi J}\sin^{-1}\{\sqrt{(f_1 - f_2)^2 - 2(f_1 + f_2) + 1} - (f_1 - f_2)\} \quad [10a]$$

$$\Delta\varphi_S = \frac{\pi}{2} - \sin^{-1}\{\sqrt{(f_1 - f_2)^2 - 2(f_1 + f_2) + 1} + (f_1 - f_2)\}. \quad [10b]$$

Given that theoretical relaxation calculations cannot be expected to be sufficiently accurate to establish the exact θ_I and ϕ_S to use for a new protein they are likely to be set empirically based on experience with similar proteins. Clearly, the f_1 and f_2 values required might not be exactly the same for all sites in the protein but for practical use there is a simple rule of the thumb: Given a ±5% variation in the $^1J_{NH}$ coupling constants, the clean TROSY experiment of Fig. 4a *always* reduces the size of the semi-TROSY artifacts in cross peaks where the artifact amplitudes exceed 50% of the f_1 and f_2 values chosen for the pulse sequence. Should there be a larger deviation in the artifact amplitudes, the experiment in Fig. 4b provides an easy remedy if a slightly longer pulse sequence is acceptable. It eliminates the F_1 semi-TROSY artifacts by not exciting them by the preparation sequence using a modified S^3E element (*8, 10–12*). Then the F_2 semi-TROSY artifacts can either be ignored because they are very small (*5*) or the phase φ_S can be adjusted to suppress them.

Two different proteins were chosen for experimental demonstration, ^{15}N-labeled RAP 17–97 (N-terminal domain of α_2-macroglobulin receptor associated protein) (*13*) and the 20-kDa equinatoxin II (EQT) from the Mediterranean anemone *Actinia equina* (*14*).

First, Fig. 5a shows an overview of the ^{15}N–^{1}H correlation in RAP taken with the clean TROSY sequence of Fig. 4a. The framed region from different spectra is expanded in the figure: Fig. 5b is from the conventional uncompensated TROSY spectrum exhibiting semi-TROSY artifacts; 5c and 5d are clean TROSY spectra recorded with the sequences in Figs. 4a and 4b, respectively. It is evident from the sections shown that the

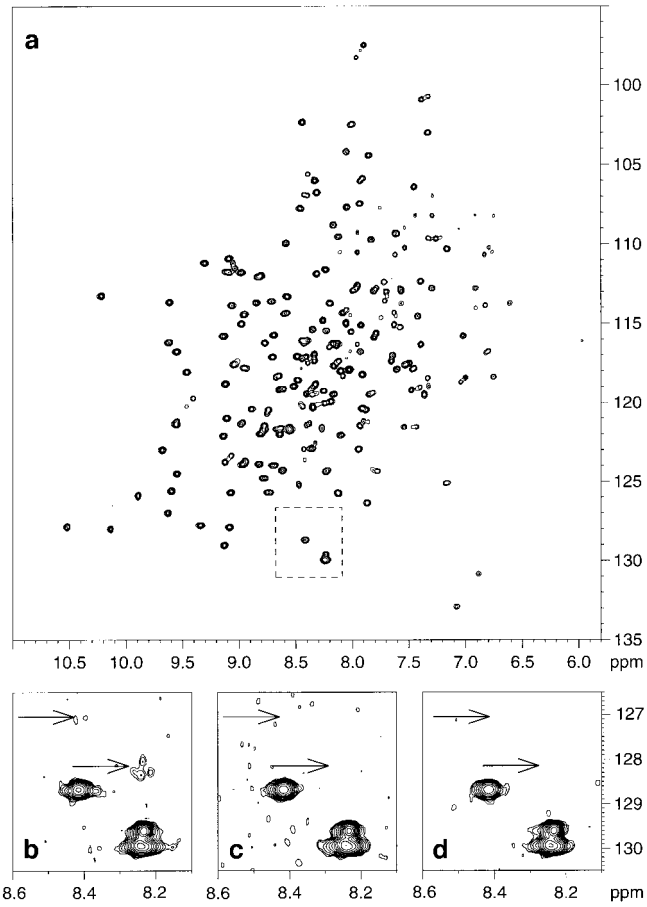

FIG. 6. ^{15}N–^{1}H clean TROSY spectra of the 20-kDa equinatoxin from the Mediterranean anemone *Actinia equina* (90%/10% H_2O/D_2O, 300 K) recorded on a Bruker DRX 600. The dashed region in the overview (a) is expanded in the subsequent panels: (b) conventional TROSY spectrum, i.e., using the sequence of Fig. 4a with the parameters $\tau = \tau_I = \tau_S = (2J_{NH})^{-1} = 5.21$ ms and $\varphi_I = \varphi_S = \pm y$ in the antiecho/echo selection. Here the F_1 semi-TROSY peaks are clearly visible (see arrows) while the F_2 ones are not. The clean TROSY spectrum in (c) was recorded with the setting $\tau = \tau_S = (2J_{NH})^{-1} = 5.21$ ms, $\tau_I = 3.47$ ms (corresponding to $\theta_I = \pi J_{NH}\tau_I = 60°$ for $J_{NH} = 96$ Hz) and $\varphi_I = \pm y$ and $\varphi_S = 86°, -94°$ for antiecho/echo. (d) shows the clean TROSY spectrum recorded with the sequence of Fig. 4b employing the parameters $\tau_F = 2.31$ ms and $\varphi_F = 50°$. The other ones are $\tau_I = \tau_S = (2J_{NH})^{-1} = 5.21$ ms, $\varphi_I = \pm y$, and $\varphi_S = 86°, -94°$. In all cases 32 scans were recorded with 256 echo and antiecho increments in t_1 and 2048 data points in t_2 in the conventional alternating antiecho/echo mode. Spectral widths are 15 ppm in F_2 (on-resonance for water) and 50 ppm in F_1. Zero-filling to 8k (t_2) by 4k (t_1) data points prior to strip transformation was done for the spectral regions shown while apodization employed a $\cos^2$ window function shifted by 18° in both dimensions. Gaussian water-selective $\pi/2$ pulses of 750-μs duration were used in the Watergate element.

undesired semi-TROSY artifacts are well suppressed in the clean TROSY spectra.

Figure 6a presents an overview of the correlation in the 20-kDa protein EQT using clean TROSY. In the expansions of the region indicated, the conventional TROSY spectrum presented in Fig. 6b exhibits F_1 semi-TROSY artifacts, while none are visible in F_2. Clearly, the clean TROSY experiment (Fig. 6c) suppresses the semi-TROSY artifacts, as does the clean TROSY variant applying the S^3E filter (Fig. 6d).

In conclusion, clean TROSY experiments have been derived to eliminate the undesired multiplet components (semi-TROSY peaks) occurring in conventional TROSY spectra. Two parameters in the two spin-state-selective coherence transfer elements of the TROSY mixing sequence can be adjusted to different sizes of the artifacts. Alternatively, a clean TROSY variant with an additional S^3E filter prior to t_1 can be used for cases where the artifacts in F_1 or the effective coupling constants including scalar and residual dipolar contributions vary strongly.

Note added in proof. M. H. Levitt and O. G. Johannesen, *J. Magn. Reson.* **142,** 190–194 (2000), indicate a further reason for spectrometer-dependent signs of phase shifts.

ACKNOWLEDGMENT

The ^{15}N-RAP and EQT samples are courtesy of Flemming M. Poulsen and Poul Erik Hansen, respectively.

REFERENCES

1. R. H. Griffey and A. G. Redfield, *Q. Rev. Biophys.* **19,** 51–82 (1987).
2. K. Pervushin, R. Riek, G. Wider, and K. Wüthrich, *Proc. Natl. Acad. Sci. USA* **94,** 12366–12371 (1997).
3. K. Pervushin, R. Riek, G. Wider, and K. Wüthrich, *J. Am. Chem. Soc.* **120,** 6394–6400 (1998).
4. M. Goldman, *J. Magn. Reson.* **60,** 437–452 (1984).
5. M. Rance, J. P. Loria, and A. G. Palmer, *J. Magn. Reson.* **136,** 92–101 (1999).
6. M. D. Sørensen, A. Meissner, and O. W. Sørensen, *J. Biomol. NMR* **10,** 181–186 (1997).
7. A. Meissner, T. Schulte-Herbrüggen, J. Briand, and O. W. Sørensen, *Mol. Phys.* **95,** 1137–1142 (1998).
8. A. Meissner, T. Schulte-Herbrüggen, and O. W. Sørensen, *J. Am. Chem. Soc.* **120,** 7989–7990 (1998).
9. M. H. Levitt, *J. Magn. Reson.* **126,** 164–182 (1997).
10. A. Meissner, J. Ø. Duus, and O. W. Sørensen, *J. Magn. Reson.* **128,** 92–97 (1997).
11. A. Meissner, J. Ø. Duus, and O. W. Sørensen, *J. Biomol. NMR* **10,** 89–94 (1997).
12. A. Meissner, T. Schulte-Herbrüggen, and O. W. Sørensen, *J. Am. Chem. Soc.* **120,** 3803–3804 (1998).
13. P. R. Nielsen, L. Ellgaard, M. Etzerodt, H. C. Thøgersen, and F. M. Poulsen, *Proc. Natl. Acad. Sci. USA* **94,** 7521–7525 (1997).
14. W. Zhang, P. E. Hansen, M. G. Hinds, R. S. Norton, and G. Anderluh, personal communication.